VALIDATION TECHNIQUE FOR REMOTE SENSING PRODUCTS OF INLAND WATER QUALITY

Suhyb Salama[1], Wouter Verhoef[1], Jaak Monbaliu[2], Zoltan Vekerdy[1], Chris Mannaerts[1] and Bob Su[1]

1. *International Institute for Geo-Information Science and Earth Observation , The Netherlands*
salama@itc.nl

2. *Hydraulics laboratory , Katholieke Universiteit Leuven, Belgium*
jaak.monbaliu@bwk.kuleuven.be

ABSTRACT

Remote sensing of water quality is initiated as an additional part of the on going activities of the EAGLE2006 project. Within this context intensive in-situ and airborne measurements campaigns were carried out over the Wolderwijd and Veluwemeer natural waters. However, in-situ measurements and image acquisitions were not simultaneous. This poses some constraints on validating air/space-borne remote sensing products of water quality. Nevertheless, the detailed in-situ measurements and hydro-optical model simulations provide a bench mark for validating remote sensing products. That is realized through developing a stochastic technique to quantify the uncertainties on the retrieved aquatic inherent optical properties (IOP).
The output of the proposed technique is applied to validate remote sensing products of water quality. In this processing phase, simulations of the radiative transfer in the coupled atmosphere-water system are performed to generate spectra at-sensor-level. The upper and the lower boundaries of perturbations, around each recorded spectrum, are then modelled as function of residuals between simulated and measured spectra. The perturbations are parameterized as a function of model approximations/inversion, sensor-noise and atmospheric residual signal. All error sources are treated as being of stochastic nature. Three scenarios are considered: spectrally correlated (i.e. wavelength dependent) perturbations, spectrally uncorrelated perturbations and a mixed scenario of the previous two with equal probability of occurrence. Uncertainties on the retrieved IOP are quantified with the relative contribution of each perturbation component to the total error budget of the IOP.
This technique can be used to validate earth observation products of water quality in remote areas where few or no in–situ measurements are available.

INTORDUCTION

Due to the stochastic nature of measurements, and corrections (e.g. atmospheric correction), the retrieved water leaving reflectance is not the only possible spectrum [1]. Instead, there are many other spectra (i.e. hypothetical spectra) of the water leaving reflectance. Each one of these hypothetical spectra has the same probability of being the measured water leaving spectrum. Therefore a different set of water inherent optical properties (IOP) would have resulted if a hypothetical spectrum had been realized. In consequence, the hypothetical-IOP (i.e. resulting from inverting the hypothetical spectra) will have a certain probability distribution from which the solution vector IOP_0 was drawn. Equivalently the difference between the solution vector IOP_0 (our first estimates) and the true IOP is one member drawn from the probability distribution of the differences between the hypothetical-IOP and the true IOP. This distribution (of the differences) provides all the necessary information about the quantitative uncertainties in the solution vector IOP_0 [2].
The first objective of this study is to estimate this distribution and evaluate the relative contribution of each perturbation-component to the total error of IOP. This is done by separating the influence of these fluctuations on the retrieved IOP. This will provides us with the necessary tool to quantify the sensitivity and the uncertainties of the IOP to fluctuations in the recorded spectrum. The second objective is to assess the quality of three remote sensing reflectance products (space-borne, airborne and ins-situ) in retrieving the IOP of the water column.

METHOD AND DATA

Remote Sensing Modelling

The total recorded radiance $L_t\left(\vec{X},\theta_0,\theta,\phi-\phi_0,\lambda\right)$ at the sensor level is converted to reflectance $\rho_t^{(\lambda)}$ at wavelength λ [3]:

$$\rho_t^{(\lambda)} = \frac{\pi L_t\left(\vec{X},\theta_0,\theta,\phi-\phi_0,\lambda\right)}{\cos\theta_0 E_0^{(\lambda)}} \quad \textbf{(1)}$$

Where θ_0,θ are the sun and sensor zenith angles respectively with relative azimuth angle of $(\phi-\phi_0)$. The term $E_0^{(\lambda)}$ is the extraterrestrial solar irradiance. The viewing-geometry of all reflectance terms will be dropped for brevity.
The total received reflectance at the sensor level can be written as the sum of several components:

$$\rho_t^{(\lambda)} = tg^{(\lambda)}\left(\rho_a^{(\lambda)} + \rho_r^{(\lambda)} + \rho_{ra}^{(\lambda)} + tv^{(\lambda)}\left(\rho_{sfc}^{(\lambda)} + \rho_w^{(\lambda)}\right)\right) \quad \textbf{(2)}$$

Where *tg* and *tv* are gaseous transmittance and viewing diffuse-transmittance from ocean to sensor, respectively. The subscript of the reflectance represents the contribution from surface (*sfc*) aerosol (*a*), air molecules (*r*), coupled scattering (*ra*) and the water leaving reflectance (*w*). The calculation of Rayleigh scattering of air molecules is well described in terms of geometry and pressure [4]. Sea surface reflectance can be estimated using statistical relationships and wind speed [5] and [6]. Gaseous transmittance can be calculated from ancillary data on ozone and water vapor concentrations using the transmittance models of [7] and [8]. Viewing diffuse transmittance is approximated following [9]. Aerosol multiple-scattering component can be measured using a hand held or fixed sun-photometer. This information facilitates the retrieval of the water leaving reflectance from the total recorded signal. The water leaving reflectance can then be related to the water physical and biological properties as follows [10]:

$$\frac{\rho_w^{(\lambda)}}{T_o^{(\lambda)}} = 0.54\pi l_1 \frac{b_b(\lambda)}{b_b(\lambda)+a(\lambda)} \quad \textbf{(3)}$$

Where $\rho_w^{(\lambda)}$ is the water leaving reflectance normalized to the solar transmittance from sun-to-target $T_o^{(\lambda)}$; $l_1 = 0.0949$ is a subsurface expansion coefficient due to internal refraction, reflection and sun zenith. The parameters $b_b(\lambda)$ and $a(\lambda)$ are the bulk backscattering and absorption coefficients of the water column (subset of the water inherent optical properties IOP). These IOP characterize the optical behavior of the medium and are directly related to the concentrations of water constituents. The values of IOP can be quantified by inverting the above model (equation 3) using non-linear fitting [11]. The assumed water constituents are chlorophyll-a (phytoplankton green pigment, Chl-a), dissolved organic matter (DOM) and suspended particulate matter (SPM). The IOP of these constituents are then parameterized following [12], [13] and [14] for Chl-a, DOM and SPM, respectively. Note that the absorption and backscattering coefficients of any constituent are linearly related to its concentration. Therefore we refer to both parameters (concentration and absorption/ backscattering coefficient) using the same abbreviation of the constituent itself (i.e., DOM, Chl-a, SPM).

Study Area and Dataset

Field measurements of water leaving reflectance, turbidity and Chlorophyll-a of the Wolderwijd and Veluwemeer (52º19'12.0"N, 05º36'12.0"E.) natural waters were available from Eagle2006 campaign for the 4th of July 2006. This filed campaign was also associated with hyperspectral airborne measurements form the Airborne Hyperspectral Spectrometer (AHS) [15]. MEdium Resolution Imaging Spectrometer (MERIS) and Advanced Space borne Thermal Emission and Reflection Radiometer (ASTER) observations were also available during the EAGLE2006 campaign. For more details on EO data availabilities and specifications the reader is encouraged to consult the Eagle2006 data acquisition report [16],. Table (1) summarized the used dataset in this work.

Table 1: Summary of the subset from Eagle2006 dataset used in this study.

Acquisition	Sensor	Description	Date
Space borne	MERIS	MER-FR-PNEPA20060608_101603_000000502048_00237_22335_1597.N1	08-06-2006
	ASTER	AST_L1B_00306082006104429_20060706063029_30252.hdf	08-06-2006
Airborne	AHS	AHS_060613 level L1b	13-06-2006
Field measurements	ASD	9 Spectra: corrected for sky reflectance using the NIR spectrum	04-07-2006

RESULTS AND DISCUSSIONS

Error Propagation and Quantification

Accuracy of Model-Inversion and Sensitivity Analysis

Water leaving spectra are produced for a set of synthesized values of water IOP using equation (3). These spectra are then inverted to retrieve the water IOP. The deviations between retrieved and synthesized values of IOP are measures of model-inversion accuracy. The relative errors in the retrieved IOP are quantified and shown in fig.1-a for each water type. Two important observations can be drawn from fig.1. The first is that the model is very appropriate for SPM retrieval with a maximum relative error less than 0.02%. This value (of 0.02%) decreases with increasing SPM concentrations to reach maximum value less than 0.005% at 30 $g.m^{-3}$ of SPM. The second observation is that the relative-error in Chl-a increases with increasing the concentrations of DOM. This is more pronounced at low concentrations of Chl-a and SPM. The relative-error of DOM increases with increasing DOM and decreasing SPM and Chl-a concentrations. In general the concentrations of Chl-a are overestimated in waters with low concentrations of DOM and underestimated in waters with high concentrations of DOM. The sensitivity of the Chl-a to the abundance of DOM could be due to a degeneracy effect of the inversion. This might explain why case II waters with high concentrations of DOM (absorption at 440nm $\geq$ 0.25) were avoided in most coastal studies by assuming a small constant value of DOM absorption coefficient [17]. Let us note that the spectral-slop of DOM absorption can also be retrieved through the inversion. Nevertheless this will increase the degrees of freedom and hence the degeneracy of the solution. However the algorithm (as it was presented) succeeded in reproducing very good estimates of the IOPs. The relative errors were less than 0.05% in DOM, less than 0.018% in SPM and less than 1.8% in Chl-a.

The sensitivity of model-inversion to fluctuations in the water leaving reflectance is quantified as being the deviation of errors (resulting from fluctuations) from minimum errors (when no fluctuation was considered). This deviation is computed for 1000 fluctuated spectra and shown in fig.1-b. The accuracy of the retrieved Chl-a, DOM and SPM concentrations increased with increasing the concentrations of SPM. This trend was inverted for DOM. i.e. the accuracy of the IOP decreased with DOM abundance.

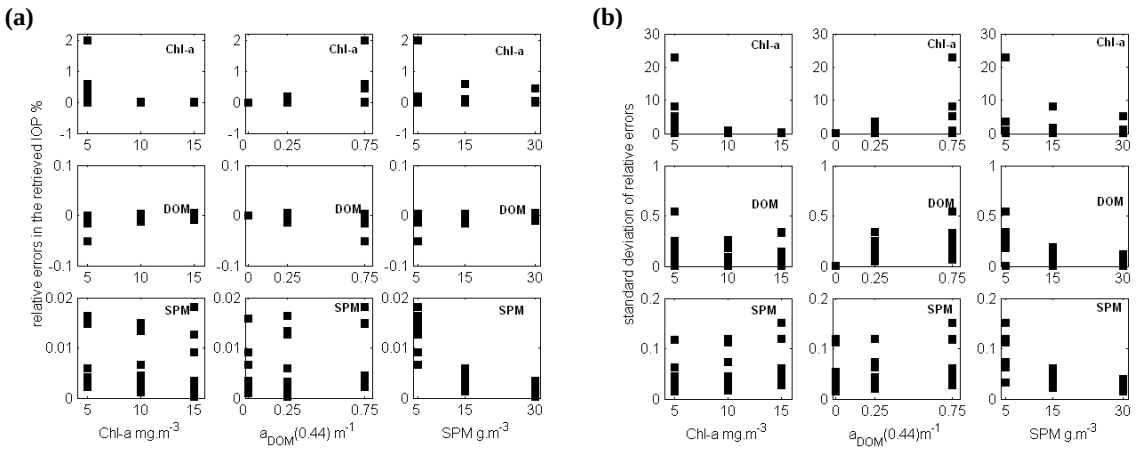

Fig.1: (a) Errors in the estimated IOP; (b) Standard deviations (retrieved form 1000 fluctuated spectra).

For DOM free water, the relative errors in the estimated concentrations of Chl-a and SPM increased over clear waters. It appears from fig.1-b that the absorption coefficient of Chl-a is the most sensitive parameter to the random fluctuations in the water leaving reflectance. This is true if DOM is presented in the water. In this case, the retrieved concentrations of Chl-a have 65% probability to be within $\pm 23\%$ off the true values. For DOM-free water this uncertainty in the retrieved concentrations of Chl-a is reduced to less than 0.2% for the same probability of occurrence. These conclusions are correct with respect to the associated range of spectral fluctuations.

Upper and Lower Bounds

Residuals between model predications and measurements are used to construct upper and lower bound on the estimated IOP following [18] and [19]. The upper and lower bound are shown in fig.2-a. The fits between molded and measured reflectance are within acceptable ranges. The maximum norm of residuals is equal to 3.8. This is not the case for sites 3 and 4, where bottom reflectance was observed. At these two sites the norm of residuals is 10.6 and 5.5 respectively.

Imperfect Atmospheric Correction and Sensor's Noise

Errors in aerosol optical thickness are assumed to be between 0.17 and 0.26. These values correspond to an urban atmosphere model with visibilities between 40 km and 20km, respectively. These two values are used to generate upper and lower bounds of water leaving reflectance. Any value of aerosol optical thickness will result in a different water leaving spectrum. These spectra are then generated within the upper and lower bounds randomly.

Random noise is assumed to follow a normal distribution with zero mean and $\alpha \times$(noise equivalent radiance) of a sensor. This number depends on sensor specifications and the desired confidence interval.

The relative contribution of each error source to the total errors on the IOP is then calculated using the variances of the different error components. Fig.2-b shows that model inversion and imperfect atmospheric correction are the major contributors to the uncertainties on the retrieved values of Chl-a and DOM absorption coefficients. Retrieved values of SPM are more affected by sensor noise and aerosol. This is similar to the, already, observed behavior of the inversion in twins experiment. However, the values of model inversion's errors are higher than those already noted during the twins experiment. This is due to the random nature of measurements which may disagree with the simulated randomness. In general, noise and aerosol induced uncertainties account for 60% to 75% of the total error, while model inversion account for the remaining 25% to 40% of the total error on the retrieved IOP (see table 2). Table (2) contains the averaged values of relative contributions from different sources of uncertainties over all measured sites.

The relative contribution of model inversion is at its maximum for DOM (~40%) and its minimum for SPM (25%). Noise induce errors have a small contribution to absorber (DOM~14% and Chl-a~19%) and a large contribution to scatterer (SPM~43%). More than half (~51%) of errors on the retrieved values of Chl-a are originated form imperfect atmospheric correction. This is reduced to 43% and 32% for the retrieved values of DOM and SPM respectively.

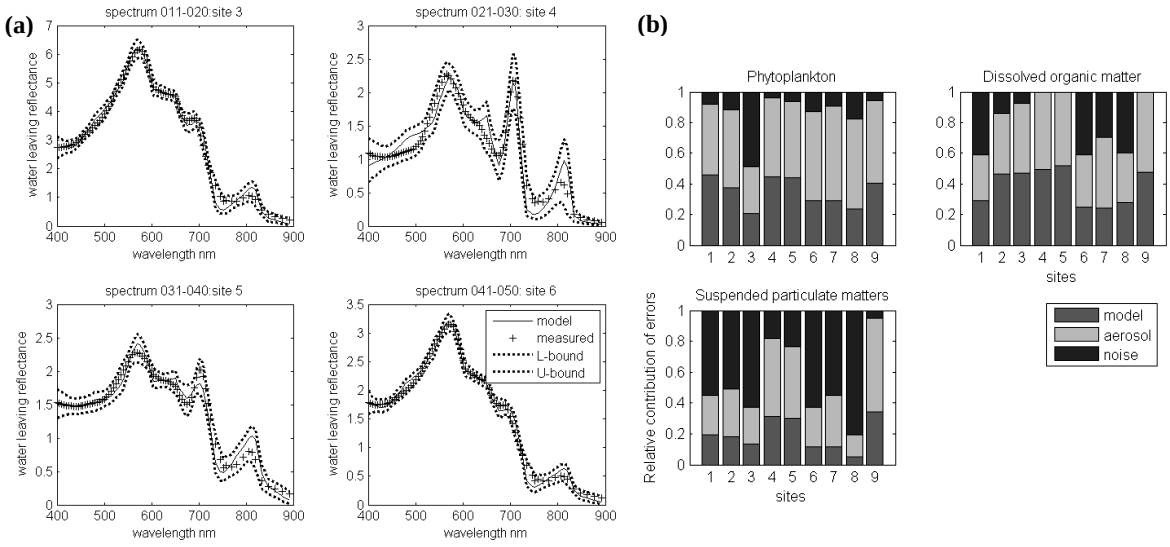

Fig.2: (a) modeled versus ASD water leaving reflectance with 99% of confidence with upper bound (U-) and lower bound (L-); (b) The relative contribution of the different errors to the total uncertainties on the IOP.

Table 2: Averaged values of relative contributions of the different sources of errors to the total budget of uncertainties on the retrieved IOP.

Relative contribution	Chlorophyll-a	Dissolve organic matters	Suspended matters
Model inversion error	35	39	25
Aerosol uncertainty	51	42	32
Sensor noise	14	19	43

Retrievals and Products Inter-comparison

Geo-referencing and Atmospheric Correction

Available images are geo-referenced, corrected for smile effects and converted to top of atmosphere reflectance. Atmospheric path correction is then preformed using radiative transfer computation [20]. Gaseous transmittances of ozone, oxygen, carbon dioxide, methane and nitrous oxide are assumed constant over a sub region of all images. Two aerosol models with 40 km visibility are used, namely maritime aerosol for MERIS and urban aerosol for AHS and ASTER. The adjacency effects form the surrounding lands is accounted for in the computation.

Retrieval of Water Quality Parameters and Products Inter-comparison

Non-linear fitting is used for simultaneous retrieval of the water IOP. This method is applied on MERIS and AHS spectra. The spectral characteristics of ASTER constrain the application of such non-linear fit method. Instead, matrix inversion method is applied on ASTER's two visible bands. In consequence only two variables were retrieved form ASTER image. An inter-comparison between retrieved values of SPM backscattering and Chl-a and DOM absorptions are shown in (fig.3) for two cross sections over the Veluwemeer (start {52.38307, 5.63710}, end {52.3681, 5.65516}) and the Wolderwijd (start {52.34515, 5.60731}, end {52.3579, 5.59198}). Retrieved values from ASTER are patchy and don't correspond to the values estimated from MERIS and AHS. This is because the retrieval-method of ASTER is based on matrix inversion of equation (3) in two bands and assuming a constant value of DOM absorption coefficient at 400nm (= 0.25 m^{-1}). The retrieval-method of MERIS and AHS is based on non-linear fit for IOP in all visible bands (i.e. 15 for MERIS and 16 for AHS). There is a very good match in the retrieved values of SPM backscattering at Veluwemeer (fi.g.3a) and Chl-a absorptions at the Wolderwijd (fig.3-d). However, slight overestimations of Chl-a absorption and underestimations of SPM backscattering coefficients w.r.t. AHS can be observed in (fig.3-b) and (fig.3-c) respectively. The values of DOM absorption coefficient are generally overestimated w.r.t AHS retrieved values, with the same spatial variation, however. The differences between MERIS and AHS results may be attributed to imperfect atmospheric correction and inappropriate spectral coverage of AHS for Chl-a retrieval. On the one hand, the longer atmospheric path of MERIS w.r.t. AHS signals increases the contributions of adjacency effects, aerosol type and illumination-viewing variations to the top of atmosphere (TOA) reflectance. On the other hand, AHS spectral range does not cover chlorophyll-a absorption feature centered at 440 nm. This absorption feature is of quite importance for reliable estimation of Chl-a and DOM absorption coefficients. The combined effects of the longer atmospheric path and the absence of 440nm absorption feature will increases the uncertainties on the retrieved values of DOM and Chl-a contributing up to 86% (the sum of relative contributions of aerosol and model inversion from table 2) to the total errors.

Validation of EO Products

Inversion's by-products are the residuals and the partial derivative of equation (3). These information are then used to estimate the uncertainty on the retrieved IOP from AHS dataset [18], [19]. Here we use the standard deviation (STD) at 95% of confidence as a measure of uncertainties. The retrieved values of DOM have the highest uncertainties (fig.4-a and fig.4-b). This was already anticipated form the pervious results (fig.3-e and fig.3-f). The uncertainty maps have similar spatial variations (fig.4-a, fig.4-c and fig.4-e) and their values increase proportionally to water turbidity. Two water types can be distinguished form the right panels of fig.4 (the surrounded region in fig.4-b, fig.4-d and fig.4-f), the pixels within the plotted region have STD values less than the value of the corresponding IOP. The remaining pixels, which form the majority, have their STD values higher than the retrieved values of IOP (i.e. large errors). Nevertheless, the STD maps, shown in the left panels of fig.4, are the only measure of retrieval reliability over remote area where few or no in–situ measurements are available.

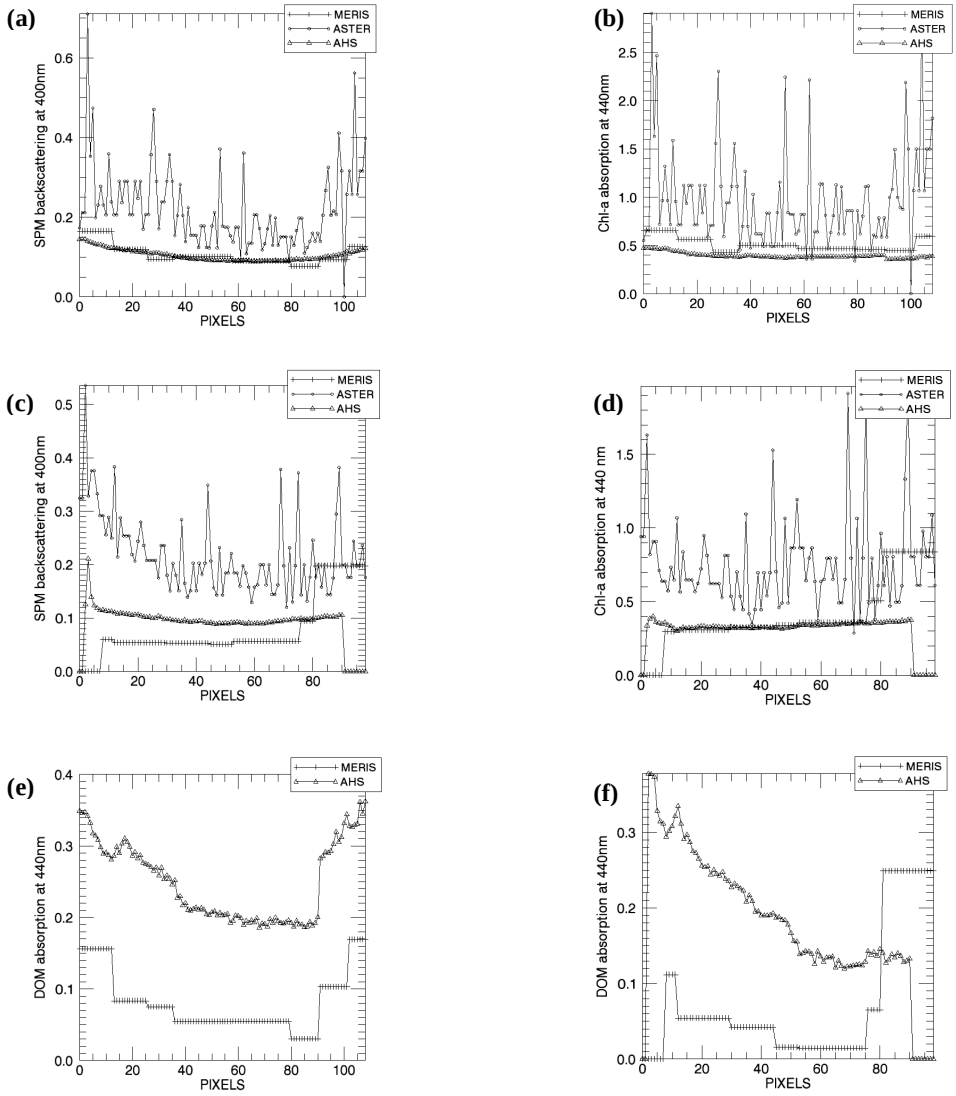

Fig.3. Inter-comparison of retrieved values of SPM (a and c), Chl-a (b and d) and DOM (e and f) from different sensors for two cross sections at the Veluwemeer (a, b and e) and Wolderwijd (c, d and f).

CONCLUSIONS

The inversion method might fail in predicting the blue and the red absorption bands of DOM and Chl-a. This is because the spectral slope of the DOM was assumed constant. Moreover the variation of the Chl-a absorption coefficient with phytoplankton species is not considered in this study.

Let us note that the inversion will only be able to separate the absorption of Chl-a from that of DOM at the blue and the red bands (centered at 440nm and 675nm respectively). Fluctuation in these two bands, will therefore, result in degenerated results of Chl-a and DOM. On the other hand SPM values are expected to be biased proportional to the residuals at the NIR.

Erroneous estimation of aerosol optical thickness and model inversion are the major source of errors. Their contribution to the total error is about 55% for SPM and 86% for DOM. Noise contribution ranges from 14% for DOM to 43% for

SPM. These observations are valid for the adapted inversion technique, non absorbing aerosol and the used noise spectral variation.
ASTER results are very patchy and their values are generally higher than those retrieved from MARIS and AHS.
There is a very good match between MERIS and AHS retrieved values of SPM backscattering and Chl-a absorption. Retrieved values of DOM absorptions coefficient from MERIS and AHS have large discrepancy. This can be attributed to the absence of the green absorption feature from AHS spectral bands and imperfect atmospheric correction. These two factors can contribute up to 86% of errors to the retrieved value of DOM.
Uncertainty maps are simultaneously estimated for each retrieved IOP. This information forms a benchmark for validation and fusion of remote sensing products of water quality parameters.

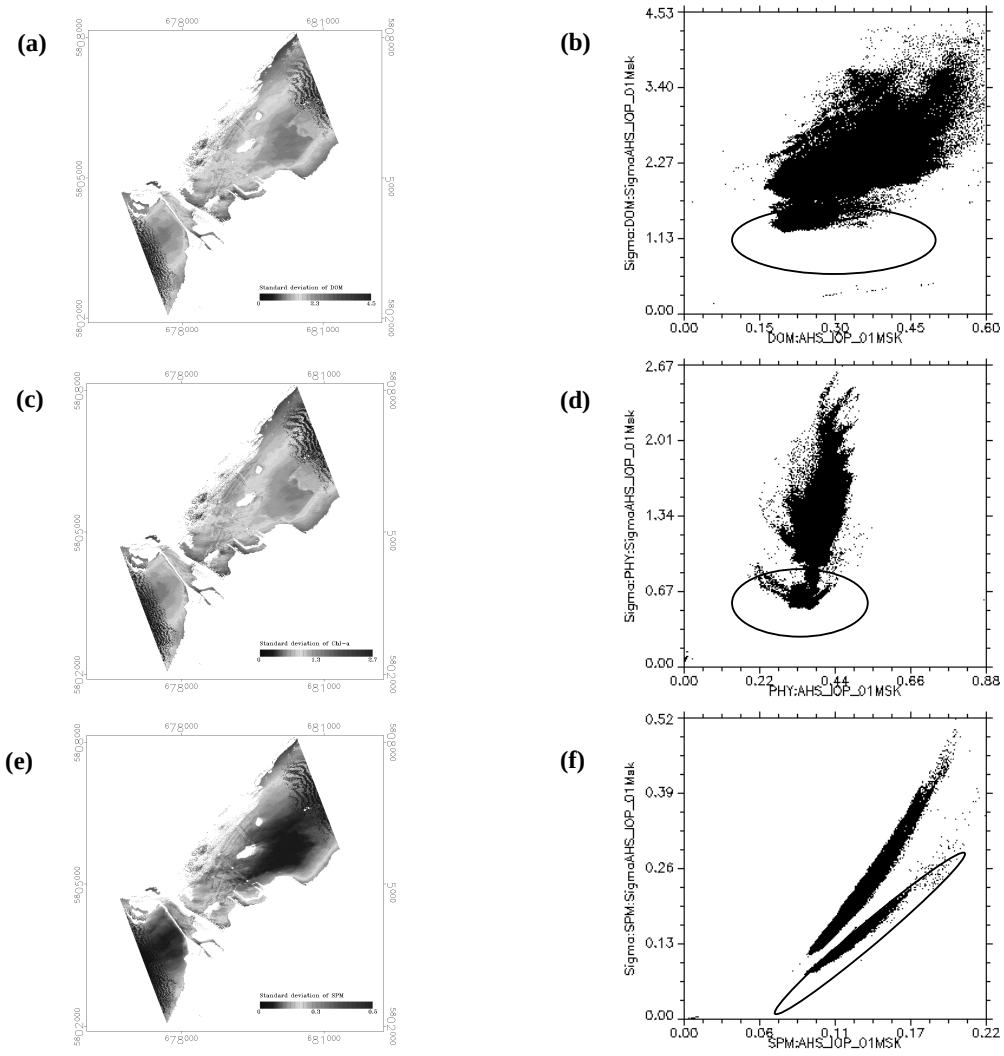

Fig.4. left panels show the standard deviation maps for each of the retrieved IOP form AHS dataset (a: DOM, c: Chla and e: SPM). Right panels (b, d, f) illustrate the scatter plot between standard deviations values (Y axis) and the corresponding IOP values (X axis).

ACKNOWLEDGMENT

The authors would like to thank The European Space Agency (ESA) for supporting this research and supplying MERIS data, The Instituto Nacional de Técnica Aeroespacial (INTA) for providing high quality hyperspectral dataset and technical assistance, The National Aeronautics and Space Administration (NASA) for providing ASTER data, The EAGLE2006 team, especially Mohammad Abouali, for collecting in-situ measurements. The financial support of ESA, arrangement No. 20239/06/I-LG, is gratefully acknowledged.

REFERENCES

[1] J. Duarte, M. Vélez-Reyes, S. Tarantola, F. Gilbes, and R. Armstrong, "A probabilistic sensitivity analysis of water-leaving radiance to water constituents in coastal shallow waters," in *Ocean Remote Sensing and Imaging*, vol. 5155: SPIE, 2003.

[2] S. Salama, "Optical Remote Sensing for the Estimation of Marine Bio-geophysical Quantities " in *Civil Engineering*, vol. Ph.D. Leuven: Katholieke Universiteit Leuven, 2003, pp. 175.

[3] H. Gordon, "Atmospheric correction of ocean color imagery in the Earth Observing System era," *Journal Of Geophysical Research*, vol. 102, pp. 17081-17106, 1997.

[4] H. Gordon, J. Brown, and R. Evans, "Exact Rayleigh scattering calculation for the use with the Nimbus-7 Coastal Zone Color Scanner," *Applied Optics*, vol. 27, pp. 862-871, 1988.

[5] C. Cox and W. Munk, "Statistics of the sea surface derived from sun glitter," *Journal of Marine Research*, vol. 13, pp. 198-227, 1954.

[6] C. Cox and W. Munk, "Measurements of the roughness of the sea surface from photographs of the sun glitter," *Journal of Optical Society of America*, vol. 44, pp. 838-850, 1954.

[7] R. Goody, *Atmospheric radiation 1, theoretical basis*: Oxford University Press, 1964.

[8] W. Malkmus, "Random Lorentz band model with exponential-tailed S^{-1} line intensity distribution function," *Journal of Optical Society of America*, vol. 57, pp. 323-329, 1967.

[9] H. Gordon, D. Clark, J. Brown, O. Brown, R. Evans, and W. Broenkow, "Phytoplankton pigment concentrations in the middle Atlantic bight-comparison of ship determinations and CZCS estimates," *Applied Optics*, vol. 22, pp. 20-36, 1983.

[10] H. Gordon, O. Brown, R. Evans, J. Brown, R. Smith, K. Baker, and D. Clark, "A semianalytical radiance model of ocean color," *Journal Of Geophysical Research*, pp. 10909-10924, 1988.

[11] Z. Lee, K. Carder, C. Mobley, R. Steward, and J. Patch, "Hyperspectral remote sensing for shallow waters: 2. Deriving bottom depths and water properties by optimization," *Applied Optics*, vol. 38, pp. 3831-3843, 1999.

[12] Z. Lee, K. Carder, C. Mobley, R. Steward, and J. Patch, "Hyperspectral remote sensing for shallow waters. 1. A semianalytical model," *Applied Optics*, vol. 37, pp. 6329-6338, 1998.

[13] A. Bricaud, A. Morel, and L. Prieur, "Absorption by dissolved organic-matter of the sea (yellow substance) in the \textscuv and visible domains," *Limnology And Oceanography*, vol. 26, pp. 43-53, 1981.

[14] V. Haltrin and G. Kattawar, "Light fields with Raman scattering and fluorescence in sea waters," Department of Physics,Texas University Technical 1991.

[15] A. Fernández-Renau, J. A. Gómez, and d. M. E., "The INTA AHS system," in *Sensors, Systems, and Next-Generation Satellites IX*, vol. 5978, *Sensors, Systems, and Next-Generation Satellites*: SPIE, 2005, pp. 471-478

[16] WRS_ITC, "Eagle2006 data acquisition report," Department of Water Resources, International Institute for Geo-Information Science and Earth Observation, ITC 2006,

[17] S. Tassan, "The effect of dissolved "yellow substance" on the quantitative retrieval of chlorophyll and total suspended sediment concentrations from remote measurements of water colour," *International Journal of Remote Sensing*, vol. 9, pp. 787-797, 1988.

[18] Y. Bard, *Nonlinear parameter estimation*: Academic Press, 1974.

[19] D. Bates and D. Watts, *Nonlinear Regression Analysis and Its Applications*: John Wiley and Sons, NY, 1988.

[20] E. Vermote, D. Tanre, J. Deuze, M. Herman, and J. Morcrette, "Second Simulation of the Satellite Signal in the Solar Spectrum, 6S: An overview," *IEEE Transactions on Geoscience and Remote Sensing*, vol. 35, pp. 675-686, 1997.